MICRO- AND NANO-MECHANICAL CHARACTERISATION AND MODELLING OF THE LOCAL MATRIX DEFORMATION IN FIBRE-REINFORCED EPOXY

N. Klavzer[1], S. Gayot[1,2], J. Chevalier[3], F. Van Loock[4], P.P. Camanho[5], B. Nysten[2] and T. Pardoen[1]

[1] Institute of Mechanics, Materials and Civil engineering (iMMC), UCLouvain, Belgium
[2] Institute of Condensed Matter and Nanosciences (IMCN), UCLouvain, Belgium
[3] Solvay S.A., 1120 Bruxelles, Belgium
[4] Polymer Technology Group, Eindhoven University of Technology, the Netherlands
[5] Department of Mechanical Engineering, University of Porto, Portugal

Keywords: *epoxy composite, DIC, AFM*

ABSTRACT

The prediction of the deformation and failure of fibre-reinforced polymer composites via bottom-up multi-scale models has become standard in the composite community. The development of accurate computational multi-scale models relies on the proper description, and thus characterisation of the individual components of the composite ply, i.e. fibres, matrix, and interfaces and interphases between the matrix and the fibres. However, the determination of the properties of these constituents at the micro/nano-scale remains a challenge. Additionally, the properties of the matrix are usually defined using continuum constitutive laws. Hence, there is a need for micro-/nano-mechanical characterisation methods to establish the matrix material response at the fibre/matrix level. These challenges place a limit on the accuracy of composite model predictions, even for simple unidirectional (UD) composites loaded in transverse compression or shear, where the matrix dominates the macroscopic deformation response of the composite. In this study, a combined experimental and numerical approach is used to characterise the individual constituents of a UD composite composed of carbon fibres and an epoxy resin. Emphasis is placed on the measurement and prediction of the constitutive response at a length scale close to the fibre diameter, where e.g. matrix size effects may exist. First, the local matrix deformation response in resin-rich pockets within UDs is probed by nanoindentation and atomic force microscopy (AFM). The extracted properties are compared with macro- and micro-scale properties of RTM6 from previous studies. Second, transverse compression tests on UD specimens are conducted inside a scanning electron microscope (SEM). The local strain field around the fibres is quantified using nano digital image correlation on a microscale region of interest (ROI). The DIC strain maps on a ROI are compared with those predicted via FEA using an established continuum model for RTM6.

1 INTRODUCTION

The field of computational micromechanics of fibre-reinforced polymer (FRP) composites needs accurate experimental validation of the matrix response at the fibre/matrix level. As bottom-up multiscale approaches are the driving force within the community for the study of advanced composite structures, it is important to rely on precise mechanical properties from the macro-scale down to the micro-scale [1]. Yet, a complete understanding of the micromechanics of FRPs is still lacking. Particularly, neglecting local property/structure variations of the matrix, size effects or the influence of an interphase around the fibres significantly limits the accuracy of failure predictions [2–4].

A few characterisation tools can be used for the study of the micromechanical behaviour of polymers and their composites. Among these, nanoindentation has received the most attention to characterise both bulk polymers and composites (thermoplastic and thermoset). Typical results show that the properties measured in confined volumes in between fibres are 15-20% than those measured in bulk samples [5–8]. Atomic force microscopy (AFM) has also been used to determine local heterogeneities within the bulk polymer or in matrix pockets to identify the presence of an interphase around the fibres [9,10]. Both these techniques provide crucial information about the local properties, however they do not allow

direct observation of the stress and strain fields at the micro scale. To overcome this, micro and nano digital image correlation (DIC) have been developed.

Micro DIC has first been applied to the study of FRPs by Canal et al. [11], and has since then by only used of few times [2,4,12,13]. The main limitation of the use of micro DIC was the inability to properly separate the strains resulting from the fibre and the matrix due to insufficiently fine speckle pattern. However, recently, we have proposed a novel nano DIC approach by improving the speckle pattern deposition method [14] to overcome this issue, relying on earlier study by Hoefnagels and co-workers [15].

In this work, we propose to combine nanomechanical characterisation techniques to highlight crucial features to be considered in micromechanical modelling. Hence, nanoindentation, AFM and a newly developed nano DIC method were applied to a carbon fibre-reinforced thermoset composite. Section 2 details the specimen preparation and characterisation techniques. Section 3 presents some results emerging from the aforementioned techniques and provides a discussion. Lastly, section 4 offer a short conclusion of this work.

2 MATERIAL AND METHODS

A thick UD carbon fibre-reinforced RTM6 slab was processed by RTM following the procedure described in [16], resulting in a final volume fraction of fibres of around 40%. Two types of samples were produced: cubic specimens for nanoindentation and AFM testing and dog-bone-shaped specimens for in-situ nano DIC tests. Additionally, small cylinders of pure resin specimens, cured in the same conditions as the composite, were also produced. In all cases, the samples were polished in the direction perpendicular to the fibres until mirror-like finish using a MultiPrep precision Polishing System (Allied High Tech Products, Inc., Ca, USA).

Nanoindentation tests were performed on pure resin specimens and resin rich pockets within the composite using an Agilent G200 nanoindenter. The indentation tests were performed with a Berkovich tip, at a rate of 0.05 s^{-1}, using the continuous stiffness measurement (CSM) mode to obtain a continuous measure of the hardness during the test. The contact area was estimated using the Oliver and Pharr method [17].

AFM analyses were performed using the PeakForce Tapping-QNM mode. Scans of size 6 x 6 μm^2 were made with a PeakForce frequency of 1 kHz and amplitude of 25 nm, resulting in images with a resolution of 47 $nm.px^{-1}$ and maximum indentation depth of 2-3 nm. Modulus maps were obtained using the built-in DMT calculation tool.

In-situ transverse compression tests were performed on the notched composite samples within a scanning electron microscope (SEM), using a Deben microtest machine equipped with a 2 kN load cell. A fine and dense speckle pattern was created using electron beam evaporation of indium using a physical vapour deposition machine, inspired by the method of Hoefnagels et al. [15]. The final average speckle size was around 10 nm. For each specimen, zones of interest of size 5.7 x 4.3 μm^2 and 11.4 x 8.6 μm^2 were observed, resulting in a pixel size of 6 and 12 nm, respectively. Images were taken at different stages during the loading of the sample up until global failure of the specimen. Care was taken to account for stress relaxation effects coming from the polymer matrix as wel as drift and charging effects due to the electron beam. A detailed description of the test procedure can be found in [14]. The open sources software Ncorr was used to perform the DIC analyses. In this work, the ideal set of parameters was a subset size of 10 pxl and a step size of 2 pxl.

Finite element analyses were made using the commercial code Abaqus [18]. The models were created using the same geometry as the observed regions of interest (ROI) during in-situ testing. Boundary conditions were defined using the measured DIC displacement at the edge of the ROI. 2D plane stress elements (CPS3) were used for the meshing. The carbon fibres were considered linear elastic. Perfect

fibre/matrix interfaces are considered. The RTM6 matrix was modelled as an rate-dependent elasto-plastic material following the mode developed and validated by Morelle [16]. A pressure-dependent yield criterion was defined using a linear Drucker-Prager model:

$$F = t + p\,tan\beta - d = 0, \tag{1}$$

where t is the yield stress, $p = \sigma_{kk}/3$ the pressure (with σ_{kk} the trace of the Cauchy stress tensor), β the friction angle and d the cohesion term. β defines the slope of the yield surface in the p-t plane while t is expressed as

$$t = \frac{\sigma_{eq}}{2}\left[1 + \frac{1}{r} - \left(1 - \frac{1}{r}\right)\left(\frac{I_3}{\sigma_{eq}}\right)^3\right], \tag{2}$$

with σ_{eq} is the von Mises equivalent stress, r the stress ratio between the yield stress under tension and compression and I_3 the third invariant of the deviatoric stress tensor. The flow rule is expressed as:

$$G = \sigma_{eq} + \frac{\sigma_{kk}}{3} tan\,\phi, \tag{3}$$

with G the flow potential and ϕ the dilation angle. Here, r = 1, β = 7.86 and ϕ = 0. The relevant material properties are listed in Table 1.

	E_{11} (GPa)	E_{22} (GPa)	E_{33} (GPa)	ν_{12}	ν_{23}	ν_{31}	Density (g.cm^{-3})
Carbon fibres	238	28	28	0.28	0.33	0.02	1.8
RTM6 matrix	3	-	-	0.34	-	-	1.14

Table 1: Elastic properties of the fibres and of the matrix.

3 RESULTS AND DISCUSSION

3.1 Nanoindentation

Nanoindentation tests were carried out to determine whether the matrix pockets within the composite show a different behaviour than the bulk resin. Figure 1 depicts the measured (a) hardness and (b) modulus evolution with the indentation depth for both the bulk resin and the UD composite. Several features can be noted. First, both hardness and modulus gradually decrease with increasing indentation depth in the low penetration regime. This is commonly observed in both bulk polymers and UD pockets and is related to the size effect that appears in polymers, particularly when the chains contain aromatic rings (i.e. RTM6) [19–21]. Afterwards, the values tend plateau off. For both the hardness and the modulus, it appears that the matrix pockets present higher values, namely 15-20 % increase. Note that the strong increase around 1µm for the modulus is cause by the presence of the fibres. This increase in property has been reported in the literature by others [5], however a clear explanation has not yet been provided. Evidence points towards an impact of aging, where an accelerated aging may occur in small matrix pockets [22]. This aspect requires further investigation.

3.2 Atomic force microscopy

To complement the nanoindentation tests and to provide information at the submicron scale, AFM measurements were made on the UD composite sample. Figure 2 (a) shows the DMT modulus map obtained using the PeakForce tapping mode. Figure 2 (b) depicts the evolution of the DMT modulus along two profiles traversing the fibre/matrix interface. A transition zone of roughly 150 nm appears around the fibres. The steady variation of the DMT modulus within this region hint towards the presence of an interphase layer between the fibre and the matrix. Yet, the presence of an interphase is typically neglecting in micromechanical models and studies providing quantitative properties about it are scarce.

Hence, it seems crucial to further characterise the formation conditions and properties of the interphase layer in FRPs.

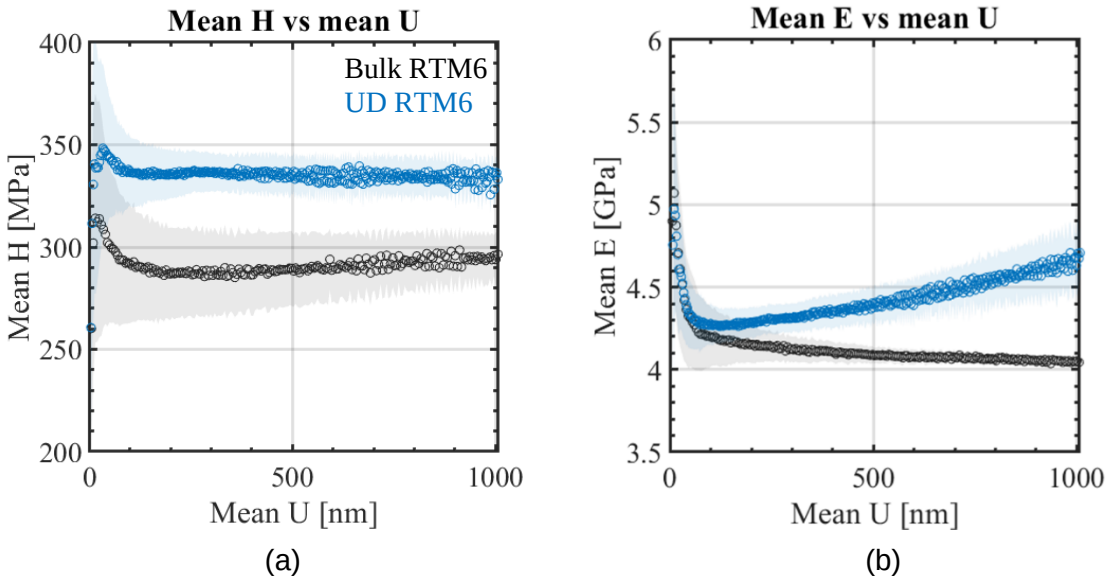

Figure 1: Nanoindentation measurements on bulk RTM6 and UD RTM6 matrix pockets - (a) hardness and (b) modulus.

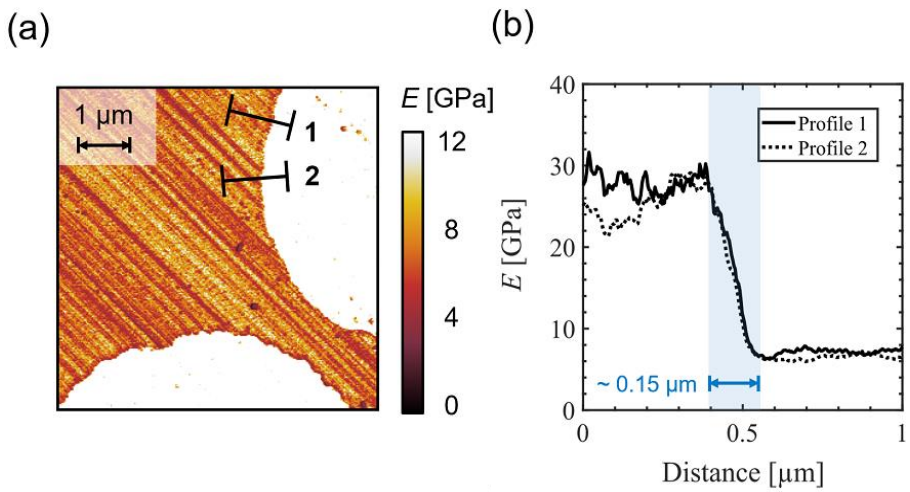

Figure 2: Atomic force microscopy measurement obtained by PeakForce tapping - (a) DMT modulus map and (b) evolution of DMT modulus along two profiles.

3.3 Nano DIC

DIC was applied to the ROI presented in Figure 3, which depicts a small material region free of any loading and right after first local failure within the ROI. The DIC analysis was performed up until the last stage before the local crack in Figure 3 (b) appeared. Figure 4 shows the corresponding strain maps for ε_{xx} and ε_{yy}. First, the novel nano DIC approach is able to accurately distinguish between the matrix and the fibres, a task that remained a challenge within the community. This capacity to clearly distinguish the phases was achieved thanks to the high-quality speckle pattern and to the minimization

of SEM-induced errors. In the strain maps, an interphase region appears to be present around the fibres. To evaluate the strain amplitude transitions between the matrix and the fibres, the strain evolution along two profiles (white dashed lines) are shown in right-hand side of Figure 4. Along both profiles, the strain within the fibres is close to 0, whereas the matrix presents high deformations as expected. Furthermore, a transition region appears between the fibre and the matrix and spread over a distance of roughly 200-500 nm. Within this region, a gradual change in strain amplitude is observed until the matrix level is reached. This region can be associated to the interphase that forms around fibres in FRPs. The comparison with the AFM results in Figure 2 shows that the interphase width is similar for both types of experiments. Naturally, slight variations in size may arise depending on the local fibre arrangement or the size of the matrix pocket [9,10,23]. Hence, the combination of AFM and DIC allow confirmation that and interphase exists around the fibres of the RTM6 composite. The advantage of the DIC is that it provides an in-situ testing method allowing to identify not only the apparent size of the interphase, but also local strain maps.

Regions of strain concentrations can also be observed, particularly in the ε_{yy} map. In addition, regions of high strain amplitudes tend to localise near and around the fibres, highlighting the importance of the DIC to precisely separate the strain in each constituent. In the ε_{yy} map, the strain concentration area captured by DIC perfectly superimposes with the loci of crack initiation after local failure within the ROI shown in Figure 3. Hence, the nano DIC approach is able to detect regions of high strains that lead to failure, and this within matrix pockets of less than 5 microns in size. For the RTM6/carbon fibre composite, local failure tends to initiate around the interfaces/interphases with no previous sign of damage. Hence, the ability of nano DIC to pinpoint interphase regions that lead to local failure provides the community with a powerful tool to validate numerical models of micron sized volumes.

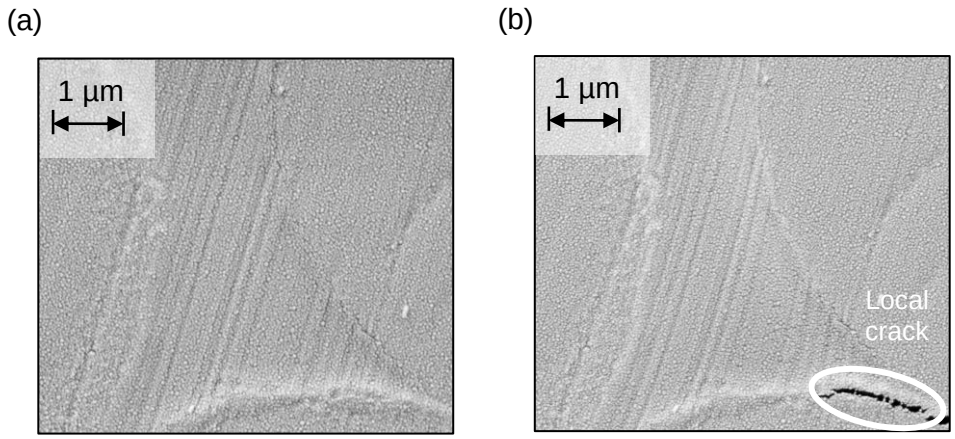

Figure 3: Comparison between initial and final (post local failure) images of the ROI. A local crack is highlighted by a white ellipse.

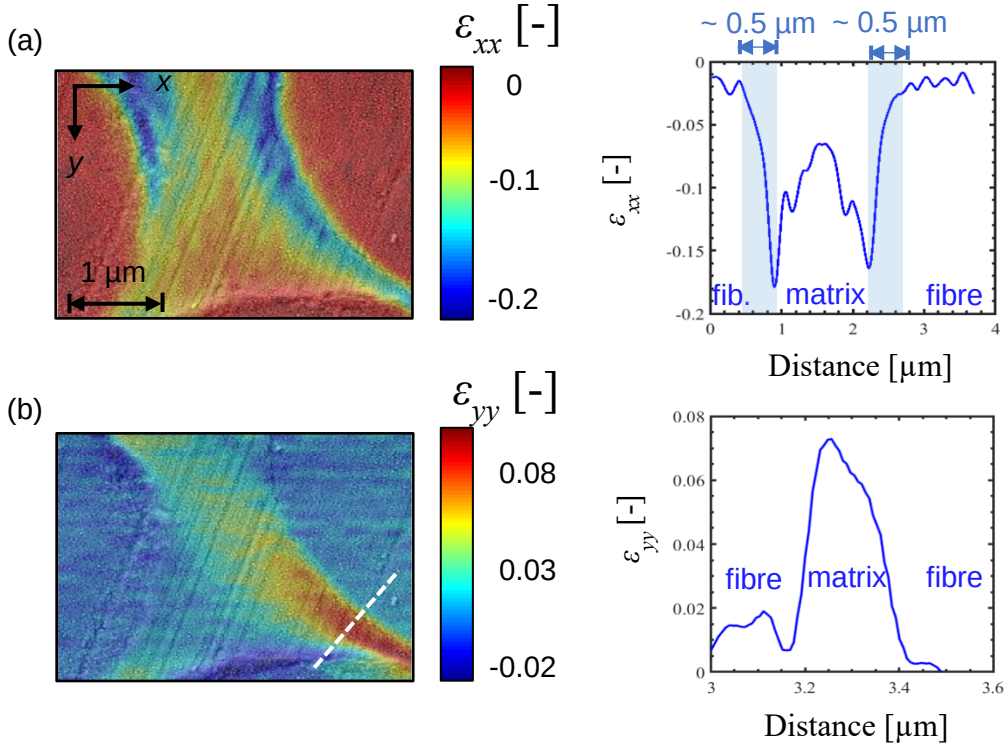

Figure 4: Strain maps and evolution of strain profiles across interfaces (white dashed lines) obtained by DIC along - (a) the *x*-direction and (b) the *xy*-direction.

3.4 Comparison to finite element analysis

Finite element analyses (FEA) were carried to re-emphasise on the inability of continuum models for the matrix to properly predict the local strain amplitudes in matrix pockets between fibres. Hence, Figure 5 (a) and (b) compares the $\boldsymbol{\varepsilon_{xx}}$ strain field measured by DIC and the one predicted by FEA. Even though the overall strain distribution is captured by FEA, the model largely overestimates the strain amplitudes around the fibres and in thin matrix strips. This is further shown in Figure 5 (c) where the strain evolution along the white dashed line are shown. This result is in line with the work of Chevalier et al. [2] who already demonstrated the inadequacy of the same continuum model when comparing with micro DIC results. Here, the main strain amplitude discrepancies are located around the fibres. Yet, the present work has shown that an interphase clearly forms around the fibres (i.e. AFM results) and that it impacts the strain accommodation within the matrix pocket (i.e. DIC). Therefore, neglecting the interphase zone in the finite element study clearly impairs the predictive capabilities of the model. Another possible explanation for the mismatch may come from possible size dependent plasticity mechanisms and effects. As the nanoindentation results have shown and as reported in the literature [19,21,24,25], size effects systematically show up within the bulk polymer but also within matrix pockets. The question remains whether this size effect is strongly affected by the interphase or not and if it is connected to strain gradient effects or to other mechanisms. Further investigations will require assessing the combined effect of both approaches.

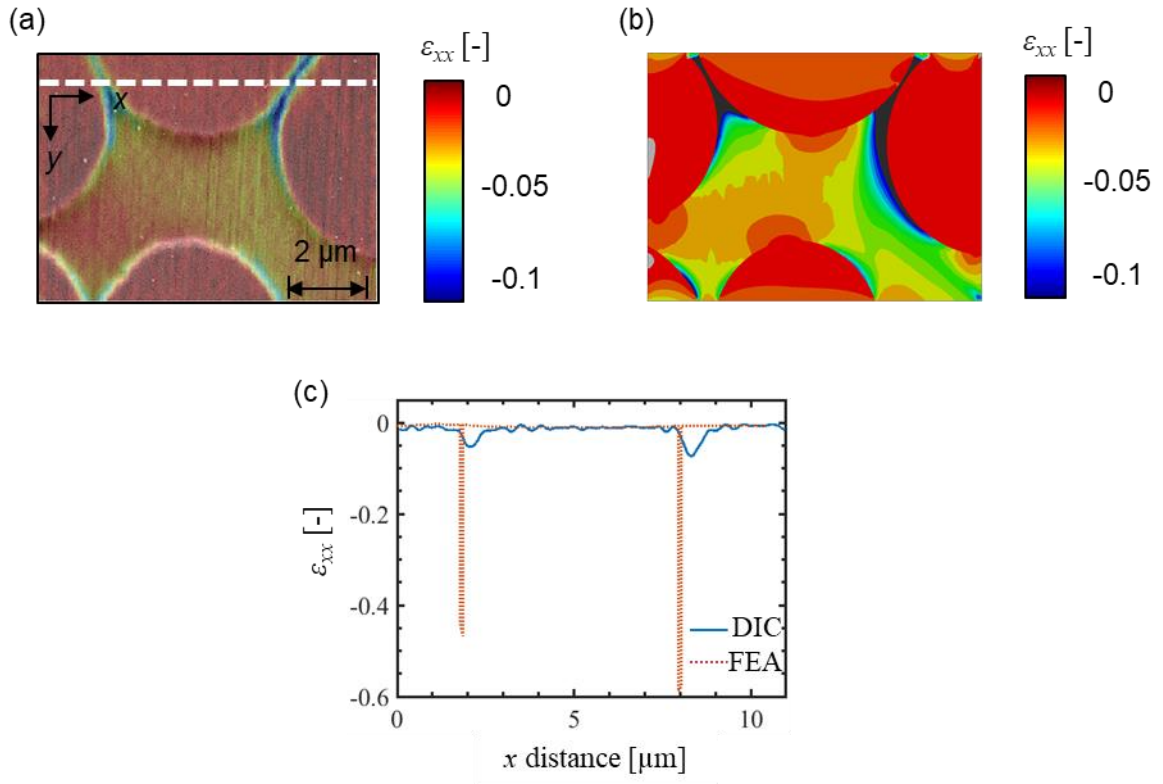

Figure 5: Horizontal $\boldsymbol{\varepsilon_{xx}}$ strain field - (a) measured by DIC and (b) predicted by FEA using a continuum model. (c) Comparison of the strain evolution along the white dashed profile for both DIC and FEA.

4 CONCLUSION

Within the framework of computational micromechanics of FRPs, accurate ply failure predictions require the understanding and quantitative determination of the local fibre/matrix level mechanical response. Furthermore, current modelling strategies lack experimental validation, especially in terms of local stress/strain fields. In this work, a micromechanical characterisation of UD thermoset composite was performed to provide additional insights into the sub-micron matrix properties. To this end, a series of micromechanical characterisation techniques were used to extract complementary information, such as the local hardness, modulus and strain fields. The main outcomes of this work are the following:

- Nanoindentation results clearly show an apparent increase of hardness and modulus within micron size matrix pockets compared to bulk results.
- Nano DIC accurately determines displacement and strains fields at the scale of a few fibres, and properly separates each constituent.
- The micro shear banding and failure patterns are captured by nano DIC, allowing its use for confronting numerical predictions to microscale experimental results.
- AFM and nano DIC confirm the systematic presence of an apparent interphase surrounding the fibres. Furthermore, the strain concentrations and failure appear to coincide with the size of the interphase, emphasising the importance of including it in micromechanical models.

Figure 5: Horizontal ε_{xx} strain field - (a) measured by DIC and (b) predicted by FEA using a continuum model. (c) Comparison of the strain evolution along the white dashed profile for both DIC and FEA.

- Finite element analyses relying on macroscale models are incapable of quantitatively describing local strain concentrations at the fibre/matrix interphase/interface.

Overall, this work shows that the local matrix behaviour at the inter-fibre level clearly differs from its macroscale behaviour. The combination of direct local strain measurements and indirect property evaluation provide strong levers to aid the micromechanics community in developing accurate models. Still, despite these efforts, the physical insights explaining this difference in behaviour are still missing. Hence, future work includes understanding the impact of curing conditions and ageing of the interphase formation and the possibility to improve numerical predictions by implementing these properties or by making use of strain gradient plasticity.

ACKNOWLEDGEMENTS

NK is a research fellow of the Fonds de la Recherche Scientifique de Belgique - FNRS and gratefully acknowledges their support. Computational resources have been provided by the supercomputing facilities of the Université catholique de Louvain (CISM/UCL) and the Consortium des Équipements de Calcul Intensif en Fédération Wallonie Bruxelles (CÉCI) funded by the Fonds de la Recherche Scientifique de Belgique (F.R.S-FNRS).

REFERENCES

[1] LLorca J, González C, Molina-Aldareguía JM, Lópes CS. Multiscale Modeling of Composites: Toward Virtual Testing … and Beyond. JOM 2013;65:215–25.

[2] Chevalier J, Camanho PP, Lani F, Pardoen T. Multi-scale characterization and modelling of the transverse compression response of unidirectional carbon fiber reinforced epoxy. Compos Struct 2019;209:160–76.

[3] Rodríguez M, Molina-Aldareguía JM, González C, LLorca J. Determination of the mechanical properties of amorphous materials through instrumented nanoindentation. Acta Mater 2012;60:3953–64.

[4] Zike S, Sørensen BF, Mikkelsen LP. Experimental determination of the micro-scale strength and stress-strain relation of an epoxy resin. Mater Des 2016;98:47–60. https://doi.org/10.1016/j.matdes.2016.02.102.

[5] Hardiman M, Vaughan TJ, McCarthy CT. A review of key developments and pertinent issues in nanoindentation testing of fibre reinforced plastic microstructures. Compos Struct 2017;180:782–98. https://doi.org/10.1016/j.compstruct.2017.08.004.

[6] Voyiadjis GZ, Malekmotiei L. Variation of the Strain Rate During CSM Nanoindentation of Glassy Polymers and Its Implication on Indentation Size Effect. J Polym Sci, Part B Polym Phys 2016;54:2179–87. https://doi.org/10.1002/polb.24127.

[7] Naya F, Micromechanics C. COMBINED MULTI-SCALE SIMULATIONS IN FIBER-REINFORCED COMPOSITES 2014:22–6.

[8] Nikaeen P, Samadi-Dooki A, Voyiadjis GZ, Zhang P, Chirdon WM, Khattab A. Effect of plastic deformation on the nanomechanical properties of glassy polymers: An experimental study. Mech Mater 2021;159:103900. https://doi.org/10.1016/J.MECHMAT.2021.103900.

[9] Bogetti TA, Wang T, VanLandingham MR, Gillespie JW. Characterization of nanoscale property variations in polymer composite systems: 2. Numerical modeling. Compos Part A Appl Sci Manuf 1999;30A:85–94.

[10] Downing TD, Kumar R, Cross WM, Kjerengtroen L, Kellar JJ. Determining the interphase thickness and properties in polymer matrix composites using phase imaging atomic force microscopy and nanoindentation. J Adhes Sci Technol 2000;14:1801–12.

[11] Canal LP, González C, Molina-Aldareguía JM, Segurado J, LLorca J. Application of digital image correlation at the microscale in fiber-reinforced composites. Compos Part A Appl Sci Manuf 2012;43:1630–8.

[12] Mehdikhani M, Aravand M, Sabuncuoglu B, Callens MG, Lomov S V, Gorbatikh L. Full-field

strain measurements at the micro-scale in fiber-reinforced composites using digital image correlation. Compos Struct 2016;140:192–201.

[13] Mehdikhani M, Matveeva A, Aravand MA, Wardle BL, Lomov S V., Gorbatikh L. Strain mapping at the micro-scale in hierarchical polymer composites with aligned carbon nanotube grafted fibers. Compos Sci Technol 2016;137:24–34. https://doi.org/10.1016/j.compscitech.2016.10.021.

[14] Klavzer N, Gayot SF, Coulombier M, Nysten B, Pardoen T. Nanoscale digital image correlation at elementary fibre/matrix level in polymer–based composites. Compos Part A Appl Sci Manuf 2023;168:107455. https://doi.org/10.1016/J.COMPOSITESA.2023.107455.

[15] Hoefnagels JPM, van Maris MPFHL, Vermeij T. One-step deposition of nano-to-micron-scalable, high-quality digital image correlation patterns for high-strain in-situ multi-microscopy testing. Strain 2019;55:12330.

[16] Morelle XP, Chevalier J, Bailly C, Pardoen T, Lani F. Mechanical characterization and modeling of the deformation and failure of the highly crosslinked RTM6 epoxy resin. Mech Time-Dependent Mater 2017;21:419–54.

[17] Oliver WC, Pharr GM. An improved technique for determining hardness and elastic modulus using load and displacement sensing indentation experiments. J Mater Res 1992;7:1564–83.

[18] ABAQUS Inc. ABAQUS/Explicit. ABAQUS Doc 2005:1–28.

[19] Chong ACM, Lam DCC. Strain gradient plasticity effect in indentation hardness of polymers. J Mater Res 1999;14:4103–10.

[20] Han C-S. Influence of the molecular structure on indentation size effect in polymers. Mater Sci Eng A 2010;527:619–24.

[21] Chandrashekar G, Han C-S. Length scale effects in epoxy: The dependence of elastic moduli measurements on spherical indenter tip radius. Polym Test 2016;53:227–33.

[22] Chevalier J. Micromechanics of an epoxy matrix for fiber reinforced composites : experiments and physics-based modelling. Université catholique de Louvain, 2018.

[23] Munz M, Sturm H, Schulz E, Hinrichsen G. The scanning force microscope as a tool for the detection of local mechanical properties within the interphase of fibre reinforced polymers. Compos Part A Appl Sci Manuf 1998;29:1251–9.

[24] Alisafaei F, Han C-S, Lakhera N. Characterization of indentation size effects in epoxy. Polym Test 2014;40:70–8.

[25] Jebahi M, Forest S. Scalar-based strain gradient plasticity theory to model size-dependent kinematic hardening effects. Contin Mech Thermodyn 2021;33:1223–45. https://doi.org/10.1007/s00161-020-00967-0.